Thermodynamic and Kinetic Aspects of Two- and Three-Electron Redox Processes Mediated by Nitrogen Atom Transfer

L. Keith Woo,* James G. Goll, Donald J. Czapla, and J. Alan Hays

Contribution from the Department of Chemistry, Iowa State University, Ames, Iowa 50011.
Received April 12, 1991

Abstract: Treatment of (*meso*-tetra-*p*-tolylporphyrinato)manganese(V) nitride, (TTP)Mn≡N, with (octaethylporphyrinato)manganese(II), Mn(OEP), in toluene leads to the reversible transfer of the nitrido ligand between the two metal complexes to form (OEP)Mn≡N and Mn(TTP). The net result is a formal three-electron reduction of (TTP)Mn^{V}N to (TTP)Mn^{II}. This occurs with a second-order rate constant of (5.6 ± 1.2) × 10^3 M^{-1} s^{-1} to form an equilibrium mixture with K_{eq} = 1.2 ± 0.5 at 20 °C. The thermodynamic and activation parameters for this process are $\Delta H°$ = 2.0 ± 0.2 kcal/mol, $\Delta S°$ = 7.1 ± 0.6 cal/mol·K, $\Delta H^{\ddagger}$ = 9.4 ± 0.7 kcal/mol, and $\Delta S^{\ddagger}$ = −10 ± 2 cal/mol·K. In THF at 20 °C, the equilibrium constant is 1.8 ± 0.2 and the rate constant drops to 2.3 ± 0.3 M^{-1} s^{-1}. When a manganese(III) porphyrin complex is used as a reductant, reversible nitrogen atom transfer still occurs but mediates a formal two-electron process. At 22 °C, the exchange process between (TTP)MnCl and (OEP)Mn≡N produces (TTP)Mn≡N and (OEP)MnCl with a second-order rate constant of 0.010 ± 0.007 M^{-1} s^{-1} ($\Delta H^{\ddagger}$ = 19 ± 2 kcal/mol and $\Delta S^{\ddagger}$ = −3 ± 6 cal/mol·K) and forms an equilibrium mixture with K_{eq} = 24.3 ± 3.3 ($\Delta H°$ = −7.0 ± 0.6 kcal/mol and $\Delta S°$ = −17 ± 2 cal/mol·K). Evidence for the formation of a binuclear μ-nitrido intermediate is presented for both processes. For the two-electron redox reaction, kinetic studies and mechanistic probes support a pathway which involves an initial chloride dissociation from the Mn(III) complex. Nitrogen atom transfer subsequently occurs between the Mn≡N complex and the four-coordinate Mn(III) cationic species.

Introduction

Although electron-transfer reactions have been intensively studied for over 40 years, our understanding of these processes is still far from complete. Particularly noteworthy in this regard is the fact that most redox reactions typically involve a one-electron change or a series of one-electron steps. Multi-electron-transfer processes which occur in a single step are exceedingly uncommon in comparison. A unique example that may fall into this category is the net four-electron process in which treatment of $W^{II}Cl_2(PMePh_2)_4$ with ketones or imines produces tungsten(VI) oxo- or imidoalkylidene complexes.[1]

One-electron redox reactions can occur by either an inner-sphere or outer-sphere mechanism. However, for multi-electron reactions, few are reported to proceed via an outer-sphere mechanism in which all electrons are transferred in the same step.[2,3] A difficulty in these outer-sphere cases involves distinguishing the single-step, multi-electron pathway from a process consisting of a series of sequential one-electron steps. Most redox reactions which involve a multi-electron step seem to be atom-transfer processes.[4] One rationale for this observation stems from the fact that multi-electron changes often are attended by drastic structural reorganization of the first coordination spheres of the reactants. Atom transfer between the two partners serves to correlate nuclear motions, providing a facile pathway for multi-electron transfer.

The best known examples of multi-electron transfer involve oxidative addition/reductive elimination reactions.[5] These types of reactions fall in the category of cross reactions. Fundamental aspects of these reactions can be obscured because a thermodynamic driving force exists. Thus, self-exchange processes are of great interest because $\Delta G° = 0$ and the intrinsic reactivities of the reactants are reflected in the rate constants and the variations in rate constants. Self-exchange reactions involving multi-electron atom-transfer redox couples have only been observed in three principal systems. One of the first recognized two-electron inner-sphere processes was the Pt(II)/Pt(IV) exchange discovered by Basolo et al. (eq 1).[6] In this example, ^{14}C-labeled ethylene-

$$trans\text{-}Pt(^{*}en)_2Cl_2^{2+} + Pt(en)_2^{2+} \rightleftarrows Pt(^{*}en)_2^{2+} + trans\text{-}Pt(en)_2Cl_2^{2+} \quad (1)$$

diamine (*en) was used as a probe to monitor the exchange. Taube and co-workers have demonstrated that halogen atom transfer can mediate a two-electron exchange between metallocenes of ruthenium and osmium (eq 2) where M = Ru or Os, X = I or Br, and Cp = C_5H_5.[7] More recently, Schwartz, Bullock,

$$Cp_2MX^{+} + Cp_2M \rightleftarrows Cp_2M + Cp_2MX^{+} \quad (2)$$

and Creutz have studied the two-electron self-exchange reactions of $CpM(CO)_3^{-}$/$CpM(CO)_3X$ couples (M = Mo, W; X = Cl, Br, I).[8] Finally, Holm has shown that oxygen atom transfer can occur between molybdenum(IV) and molybdenum(VI) complexes. Although no true self-exchange reactions were examined, equilibrium processes which approach the self-exchange condition are possible as illustrated in eq 3 (L-NS_2 = 2,6-bis(2,2-diphenyl-2-thioethyl)pyridinate(2−) and ssp = salicylaldehyde-2-thiolatoanil).[9]

$$MoO_2(L\text{-}NS_2) + MoO(ssp)(DMF)_2 \rightleftarrows MoO(L\text{-}NS_2)(DMF) + MoO_2(ssp)(DMF) \quad (3)$$

(1) Bryan, J. C.; Mayer, J. M. *J. Am. Chem. Soc.* **1990**, *112*, 2298.
(2) (a) Dodson, R. W. In *Mechanistic Aspects of Inorganic Reactions*; Rorabacher, D. B., Endicott, J. F., Eds.; ACS Symposium Series; American Chemical Society: Washington, DC, 1982; Vol. 198, p 132. (b) Schwarz, H. A.; Comstock, D.; Yandell, J. K.; Dodson, R. W. *J. Phys. Chem.* **1974**, *78*, 488.
(3) Lappin, A. G.; Osvath, P.; Baral, S. *Inorg. Chem.* **1987**, *26*, 3089.
(4) Taube, H. In *Mechanistic Aspects of Inorganic Reactions*; Rorabacher, D. B., Endicott, J. F., Eds.; ACS Symposium Series 198; American Chemical Society: Washington, DC, 1982; Chapter 7.
(5) See, for example: Collman, J. P.; Hegedus, L. S.; Norton, J. R.; Finke, R. G. *Principles and Applications of Organotransition Metal Chemistry*; University Science Books: Mill Valley, CA, 1987; Chapter 5 and references therein.
(6) (a) Basolo, F.; Wilks, P. H.; Pearson, R. G.; Wilkins, R. G. *J. Inorg. Nucl. Chem.* **1958**, *6*, 161. (b) Johnson, R. C.; Basolo, F. *J. Inorg. Nucl. Chem.* **1960**, *13*, 36. (c) Basolo, F.; Morris, M. L.; Pearson, R. G. *Discuss. Faraday Soc.* **1960**, *29*, 80. (d) Cox, L. T.; Collins, S. B.; Martin, D. S., Jr. *J. Inorg. Nucl. Chem.* **1961**, *17*, 383.
(7) (a) Smith, T. P.; Iverson, D. J.; Droege, M. W.; Kwan, K. S.; Taube, H. *Inorg. Chem.* **1987**, *26*, 2882. (b) Kirchner, K.; Dodgen, H. W.; Wherland, S.; Hunt, J. P. *Inorg. Chem.* **1989**, *28*, 604. (c) Kirchner, K.; Dodgen, H. W.; Wherland, S.; Hunt, J. P. *Inorg. Chem.* **1990**, *29*, 2381. (d) Kirchner, K.; Han, L.-F.; Dodgen, H. W.; Wherland, S.; Hunt, J. P. *Inorg. Chem.* **1990**, *29*, 4556.
(8) Schwartz, C. L.; Bullock, R. M.; Creutz, C. *J. Am. Chem. Soc.* **1991**, *113*, 1225.
(9) Harlan, E. W.; Berg, J. M.; Holm, R. H. *J. Am. Chem. Soc.* **1986**, *108*, 6992.

0002-7863/91/1513-8478$02.50/0

A wide variety of ligands can serve as bridging groups in inner-sphere reactions. Monatomic bridges, such as the halides and oxides, are particularly versatile in terms of being able to mediate one- and two-electron processes. Although much is known about how the nature of the bridging group affects the rate of inner-sphere electron transfer,[10] it is not well understood how the bridging group influences the number of electrons involved in a redox process. Furthermore, the consideration of other monatomic bridging species such as the nitrido ligand (N^{3-}) has received little attention. To some extent, this can be attributed to the weak donor property of the nitrido lone pair of electrons ($M{\equiv}N{:}$).[11] Nonetheless, the nitride is well known as a bridging ligand in a number of stable compounds. Both symmetric and asymmetric M-N-M linkages are possible and have been the subject of a recent theoretical study.[12]

An analysis of electron transfer involving a bridging nitride indicates that several types of processes are possible. Some limiting cases are illustrated in reactions 4-7. Reaction 4 involves simple oxidative bond formation with no formal change in oxidation state.

$$L_nM^x{\equiv}N{:} + M^yL_m \rightarrow \begin{cases} L_nM^x{\equiv}N{:}{\rightarrow}M^yL_{m-1} + L & (4) \\ L_nM^{x-1}{=}N{-}M^{y+1}L_{m-1} + L & (5) \\ L_nM^{x-2}{-}N{=}M^{y+2}L_{m-1} + L & (6) \\ L_mM^{x-3} + N{\equiv}M^{y+3}L_n & (7) \end{cases}$$

The complex $(Et_2PhP)_3Cl_2Re{\equiv}N{:}{\rightarrow}PtCl_2(PEt_3)$, prepared by mixing the rhenium nitrido complex with $PtCl_2(PEt_3)_2$ in benzene, is an example of this type of situation.[13] In this case, the Pt^{II} complex is a poor reductant and no redox reaction occurs. If an appropriate reducing agent is used, reactions 5-7 are possible and represent one-, two-, and three-electron-transfer processes, respectively. Using the terminology defined by Holm,[14] eqs 5 and 6 can be considered as incomplete nitrogen atom transfer and reaction 7 represents complete nitrogen atom transfer.

In the work presented here, we focus on nitrogen atom transfer reactions of metalloporphyrin complexes. Single-electron transfer mediated by atom transfer has already been demonstrated for (TPP)CoX, where TPP is tetraphenylporphyrinato and X is Cl, Br, I, and a variety of pseudohalides,[15] for (TPP)FeCl,[16] and for (TPP)CrCl.[17] In spite of this, few studies of atom-transfer reactions of metalloporphyrins exist. Nonetheless, metalloporphyrins are well suited for atom-transfer studies for the following reasons: (1) porphyrins are fairly rigid chelates known to complex a wide range of metals in a variety of oxidation states;[18] (2) the structural integrity maintained by the porphyrin ligand over this range of metal oxidation states may allow more facile multi-electron transfer; (3) the porphyrin can serve as a powerful UV-visible[19] or ^1H NMR[20] spectroscopic probe; (4) metalloporphyrins bind many types of axial ligands, such as halide, oxide, nitride, water, and pyridine, or can remain coordinatively unsaturated; (5) porphyrin complexes are soluble in innocent, non-donor organic solvents; and (6) a large number of structurally characterized porphyrin complexes exist and should allow a systematic study which addresses fundamental issues concerning the kinetic and thermodynamic factors involved in multi-electron transfer.

We report herein thermodynamic and kinetic aspects of the first *reversible* nitrogen atom transfer reactions involving two- and three-electron exchanges.[21] Prior to our work, Groves and Takahashi discovered the first example of nitrogen atom transfer.[22] This involved an irreversible process between nitridomanganese tetratolylporphyrin, (TTP)Mn≡N, and Cr(TTP). Concomitant to our studies, Bottomley and Neely reported an additional example of irreversible nitrogen atom transfer between (TTP)CrCl and (octaethylporphyrinato)manganese nitride, (OEP)Mn≡N.[23]

Procedure

General Procedure. All manipulations of air-sensitive materials were done in a glovebox or on a high vacuum line. Toluene, tetrahydrofuran, and 2,5-dimethyltetrahydrofuran were distilled from purple solutions of sodium/benzophenone, chloroform was distilled from phosphorus pentoxide, and dichloromethane was distilled from calcium hydride. Tetratolylporphyrin, H_2(TTP),[24] and Baldwin's C_2-capped porphyrin, H_2(CAP),[25] were prepared using literature procedures. Octaethylporphyrin, H_2(OEP), was obtained from Aldrich and used without further purification. Manganese(III) porphyrin chloride and acetate complexes were prepared using Adler's method.[26] Manganese(II) porphyrins were prepared by reduction of manganese(III) porphyrins with zinc amalgam as described by Reed.[17,27] (TTP)Mn≡N and (OEP)Mn≡N were prepared by Buchler's method.[28] NMR spectra were recorded on a Nicolet NT300, Bruker WM300, or Varian VXR 300-MHz spectrometer. UV-visible data were obtained using a Cary 17 or a Hewlett-Packard HP 8452A diode array spectrophotometer.

Preparation of (TTP)MnI. (TTP)Mn(O_2CCH_3) (49 mg, 0.063 mmol) was stirred with $(CH_3)_3SiI$ (0.10 mL, 0.70 mmol) in 25 mL of freshly distilled benzene for 5 min. Evaporation of all the volatile materials under reduced pressure afforded 33 mg of (TTP)MnI (62%). Recrystallization from toluene/hexane produced a purple powder. The ^1H NMR data are similar to reported literature values.[29] UV-vis (C_6H_6): 388 (Soret), 500, 648 nm. ^1H NMR ($CDCl_3$): 8.33 (br, 8 H, *m*-H), 3.15 (br, 12 H, CH_3), -26.84 (β-H).

Preparation of (TTP)Mn($O_2CC(CH_3)_3$). A solution of (TTP)MnCl (141 mg, 0.19 mmol) and $AgClO_4$ (260 mg, 1.25 mmol) was stirred in freshly distilled THF (50 mL) for 45 min at 60 °C. $NaO_2CC(CH_3)_3$ (456 mg, 3.67 mmol) was added, and stirring was continued for 1 h. After THF was removed under reduced pressure, the residues were redissolved in 50 mL of toluene and the resulting solution was filtered. Evaporation of the toluene under reduced pressure produced a green solid (144 mg, 94%). The solid was recrystallized twice from toluene/pentane. UV-vis (CH_2Cl_2): 374, 398, 470 (Soret), 578, 614 nm. NMR ($CDCl_3$): 8.06 (br, 8 H, *m*-H), 2.97 (br, 12 H, $C_6H_4CH_3$), -19.8 (br, β-H). IR (mull): ν_{CO} = 1622 cm^{-1}. Anal. Calcd for $C_{53}H_{45}MnN_4O_2$: C, 77.16; H, 5.50; N, 6.80. Found: C, 77.38; H, 5.70; N, 6.20. MS [M^-] (*m/e*): calcd 824.3, found 824.5.

Preparation of C_2-Capped Porphyrinatomanganese Nitrido Complex, (CAP)Mn≡N. (CAP)MnCl (112 mg, 0.10 mmol) was treated with (OEP)Mn≡N (32 mg, 0.05 mmol) in refluxing CH_2Cl_2 (80 mL) for 24 h. The nitrido complexes were separated from the chloro complexes by elution with CH_2Cl_2 on an alumina (neutral) column. Excess (OEP)Mn≡N was extracted from (CAP)Mn≡N with hot pentane using a Soxhlet apparatus. (CAP)Mn≡N was recrystallized from $CHCl_3$/hexane. ^1H NMR ($CDCl_3$): 8.91 (s, 4 H, β-pyrrole H), 8.78 (s, 4 H, β-pyrrole H), 7.84 (d, 7.32 Hz, 4 H, C_6H_4), 7.75 (t, 7.5 Hz, 4 H, C_6H_4), 7.51 (d, 8.1 Hz, 4 H, C_6H_4), 7.36 (t, 7.5 Hz, 4 H, C_6H_4), 5.42 (s, 2 H,

(10) (a) Taube, H.; Myers, H.; Rich, R. L. *J. Am. Chem. Soc.* **1953**, *75*, 4118. (b) Taube, H.; Myers, H. *J. Am. Chem. Soc.* **1954**, *76*, 2103. (c) Taube, H.; Gould, E. S. *Acc. Chem. Res.* **1969**, *2*, 321. (d) Haim, A. *Prog. Inorg. Chem.* **1983**, *30*, 273.

(11) Dehnicke, K.; Strähle, J. *Angew. Chem., Int. Ed. Engl.* **1981**, *20*, 413.

(12) Wheeler, R. A.; Whangbo, M.-H.; Hughbanks, T.; Hoffmann, R.; Burdett, J. K.; Albright, T. A. *J. Am. Chem. Soc.* **1986**, *108*, 2222.

(13) Chatt, J.; Heaton, B. T. *J. Chem. Soc. A* **1971**, 705.

(14) Holm, R. H. *Chem. Rev.* **1987**, *87*, 1401.

(15) Chapman, R. D.; Fleischer, E. B. *J. Am. Chem. Soc.* **1982**, *104*, 1582.

(16) Cohen, I. A.; Jung, C.; Governo, T. *J. Am. Chem. Soc.* **1972**, *94*, 3003.

(17) Reed, C. A.; Kouba, J. K.; Grimes, C. J.; Cheung, S. K. *Inorg. Chem.* **1978**, *17*, 2666.

(18) Büchler, J. W. In *The Porphyrins*; Dolphin, D., Ed.; Academic Press: New York, 1978; Vol. 1, Chapter 10.

(19) Gouterman, M. In *The Porphyrins*; Dolphin, D., Ed.; Academic Press: New York, 1978; Vol. 3, Chapter 1.

(20) (a) Janson, T. R.; Katz, J. J. In *The Porphyrins*; Dolphin, D., Ed.; Academic Press: New York, 1978; Vol. 4, Chapter 1. (b) LaMar, G. N.; Walker, F. A. In *The Porphyrins*; Dolphin, D., Ed.; Academic Press: New York, 1978; Vol. 4, Chapter 2.

(21) Preliminary reports of this work have already appeared. (a) Woo, L. K.; Goll, J. G. *J. Am. Chem. Soc.* **1989**, *111*, 3755. (b) Woo, L. K.; Czapla, D. J.; Goll, J. G. *Inorg. Chem.* **1990**, *29*, 3915.

(22) Takahashi, T. Ph.D. Dissertation, University of Michigan, 1985.

(23) Bottomley, L. A.; Neely, F. L. *J. Am. Chem. Soc.* **1989**, *111*, 5955.

(24) (a) Adler, A. D.; Longo, F. R.; Finarelli, J. D.; Goldmacher, J.; Assour, J.; Korsakoff, L. *J. Org. Chem.* **1967**, *32*, 476. (b) Rousseau, K.; Dolphin, D. *Tetrahedron Lett.* **1974**, *48*, 4251.

(25) Almog, J.; Baldwin, J. E.; Crossley, M. J.; Debernardis, J. F.; Dyer, R. L.; Huff, J. R.; Peters, M. K. *Tetrahedron* **1981**, *37*, 3589.

(26) Adler, A. D.; Longo, F. R.; Kampers, F.; Kim, J. *J. Inorg. Nucl. Chem.* **1970**, *32*, 2443.

(27) UV-vis((OEP)Mn) (toluene): 418 (Soret), 544, 580 nm.

(28) Büchler, J. W.; Dreher, C.; Lay, K.-L. *Z. Naturforsch, B: Anorg. Chem., Org. Chem.* **1982**, *37*, 1155.

(29) (a) LaMar, G. N.; Walker, F. A. *J. Am. Chem. Soc.* **1973**, *95*, 6950. (b) LaMar, G. N.; Walker, F. A. *J. Am. Chem. Soc.* **1975**, *97*, 5103.

Table I. Equilibrium Constants for Equation 9 in Toluene-d_8

T (°C)	K
−40	0.59 ± 0.19
−20	0.66 ± 0.28
0	1.02 ± 0.30
20	1.23 ± 0.46
40	1.36 ± 0.61

capping benzene), 4.42 (m, 8 H, C(O)OCH_2CH$_2$), 4.28 (m, 4 H, C(O)OCH$_2$CH_2), 3.89 (m, 4 H, C(O)OCH$_2$CH_2). UV–vis (CH_2Cl_2): 422 (Soret), 482, 538, 572 nm. MS (FAB) (m/e): calcd for $C_{62}H_{42}N_5O_{12}Mn$ 1104.03, found 1104.1.

Equilibrium Measurements. Samples for equilibrium studies were prepared by adding stock solutions of known volume and concentration of the appropriate metalloporphyrins and Ph_3CH (internal standard) to an NMR tube and evaporating the solvent on a high vacuum line. After addition of an NMR solvent under vacuum, the tube was flame sealed under a pressure of ca. 600 Torr of nitrogen. A representative mixture was prepared with (TTP)Mn≡N (1.19×10^{-3} mmol), (OEP)Mn (7.91×10^{-4} mmol), and Ph_3CH (2.99×10^{-3} mmol) in 0.50 mL of toluene-d_8. NMR spectra were then monitored in a temperature-controlled probe until no further change was observed.

Kinetic Measurements. Metalloporphyrin complexes used in kinetic studies were recrystallized at least once prior to use. Rate data for the (POR)Mn≡N/(POR)Mn system were obtained on a UV–visible spectrophotometer equipped with a thermally regulated cell holder under a blanket of nitrogen or argon. Solutions of the metalloporphyrins were loaded into a cuvette in a glovebox, sealed with a septum, and then removed from the glovebox and placed in the spectrophotometer. In a typical run, 0.35 mL of a (TTP)Mn≡N solution (4.03×10^{-5} M in toluene), 2.95 mL of toluene, and 0.20 mL (7.79×10^{-5} M) of (OEP)Mn in toluene were added to a 10-mm cuvette. The reaction was monitored at a single wavelength. A spectrum from 350 to 700 nm was taken at the end of each run to check for the absence of (POR)Mn^{III} which may have formed by adventitious air oxidation. Kinetics data for the (POR)Mn≡N/(POR)MnX (X = Cl, I, acetate, pivalate) systems were obtained by UV–visible spectroscopy in a manner similar to that described above or by monitoring changes by ^{1}H NMR spectroscopy using samples prepared as described for equilibrium determinations. Rate constants were obtained using an integrated rate law for second-order equilibrium reactions as derived by King.[30]

$$\ln\left[\frac{\Delta}{\alpha + \Delta(1 - 1/K)}\right] = -\alpha k t + \text{constant} \qquad (8)$$

Results

Reduction of Nitridomanganese(V) Porphyrin with Manganese(II) Porphyrin. Treatment of (TTP)Mn≡N with (OEP)Mn in toluene under anaerobic conditions results in spectral changes which are consistent with the transfer of a terminally bound nitrogen ligand between two metal complexes shown in eq 9. The

$$\text{(TTP)Mn}{\equiv}\text{N} + \text{(OEP)Mn} \rightleftarrows \text{(TTP)Mn} + \text{(OEP)Mn}{\equiv}\text{N} \qquad (9)$$

UV–vis spectrum of the resulting mixture contains two new Soret bands for (TTP)Mn^{II} at 435 nm and (OEP)Mn≡N at 404 nm. The Soret bands for (TTP)Mn≡N (422 nm) and (OEP)Mn (418 nm) overlap to form a single peak centered at 420 nm and do not completely disappear, indicating that eq 9 is an equilibrium process with $K = 1.2 \pm 0.5$ at 20.0 ± 0.1 °C. The reversibility of eq 9 can be confirmed by the complementary experiment in which (OEP)Mn≡N is treated with (TTP)Mn. This generates a final UV–vis spectrum that has peak positions identical to those observed for the forward process. Since the manganese(V) nitrido complexes are low-spin d^2 and diamagnetic, it is also possible to independently establish the extent of reaction by ^{1}H NMR. This is most conveniently accomplished by monitoring the β-pyrrole proton signal of (TTP)Mn≡N (8.94 ppm) and the meso proton signal of (OEP)Mn≡N (10.29 ppm) against an internal standard, the methine proton of triphenylmethane (5.51 ppm) in toluene-d_8. Flame-sealed NMR tubes containing mixtures of (TTP)Mn≡N, (OEP)Mn, (OEP)Mn≡N, (TTP)Mn, and Ph_3CH in toluene-d_8 maintain mass balance indefinitely in terms of total nitrido complex concentration. The equilibrium constants for eq 9 over an 80° range were measured by ^{1}H NMR and are listed in Table I. The thermodynamic parameters $\Delta H° = 2.0 \pm 0.2$ kcal/mol and $\Delta S° = 7.1 \pm 0.6$ cal/mol·K were derived from this temperature dependence.

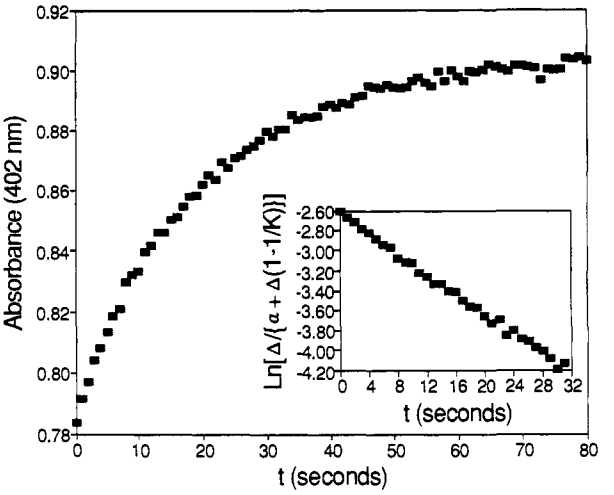

Figure 1. Representative absorption (402 nm) vs time plot for eq 9 at 20 °C. $[N{\equiv}Mn(TTP)]_0 = 5.49 \times 10^{-6}$ M, and $[Mn(OEP)]_0 = 4.83 \times 10^{-6}$ M. The inset shows a plot of ln $\{\Delta/[\alpha + \Delta(1 - K^{-1})]\}$ vs t.

The forward rates of eq 9 in toluene were examined spectrophotometrically by following the absorbance changes at 402 nm as shown in Figure 1. Kinetic runs were performed with starting concentrations ranging from 1.13×10^{-6} to 1.04×10^{-5} M and Mn≡N/Mn(II) ratios ranging from approximately 1:1 to 1:5. In all cases, the data were found to obey an integrated rate law for reversible second-order reactions (eq 8). Plots of ln $[\Delta/\{\alpha + \Delta(1 - 1/K)\}]$ vs t are linear for more than 3 half-lives. A typical plot is shown in the inset of Figure 1. Table II lists concentration data and forward and reverse rate constants for eq 9 at 20 °C, and Table III summarizes forward rate constants as a function of temperature.

A less comprehensive examination of the behavior of eq 9 in THF was also undertaken. Proton NMR studies show that, within experimental error, use of THF as solvent does not shift the equilibrium ($K_{THF} = 1.8 \pm 0.2$) at 20 °C. However, the rate of nitrogen atom transfer decreases by 3 orders of magnitude, $k_{1(THF)} = 2.3 \pm 0.3$ M^{-1} s^{-1}. Kinetic data for eq 9 in THF were also found to obey the integrated rate law, eq 8, for more than 3 half-lives. A similar set of kinetics experiments were performed at 20 °C using 2,5-dimethyltetrahydrofuran (Me_2THF) as the solvent. In this case, $k_{1(Me_2THF)} = 47 \pm 6$ M^{-1} s^{-1}.

Reduction of Nitridomanganese Porphyrins with Manganese(III) Porphyrins. (OEP)Mn≡N is also capable of transferring its terminally bound nitrogen to manganese(III) porphyrins (eq 10). This can be readily demonstrated by UV–vis or ^{1}H NMR spectroscopy using the methods discussed above. For example, the

$$\text{(OEP)Mn}{\equiv}\text{N} + \text{(TTP)MnCl} \rightleftarrows \text{(OEP)MnCl} + \text{(TTP)Mn}{\equiv}\text{N} \qquad (10)$$

UV–vis spectra of a toluene solution of (OEP)Mn≡N and (TTP)MnCl show a gradual decrease over several hours in the Soret bands of the starting nitrido (404 nm) and chloro (478 nm) complexes. New Soret bands corresponding to the formation of (TTP)Mn≡N (422 nm) and (OEP)MnCl (360 nm) simultaneously appear. In a similar fashion to eq 9, the Mn≡N/MnCl exchange process is reversible. Equilibrium constants for eq 10 in $CDCl_3$ are listed in Table IV. A plot of ln K vs $1/T$ yields $\Delta H° = -7.0 \pm 0.6$ kcal/mol and $\Delta S° = -17 \pm 2$ eu.

The high absorbance of porphyrin complexes and the slowness of eq 10 make kinetic measurements by spectrophotometric techniques impractical. However, the rate regime of eq 10 falls within the limits of the NMR time scale. Thus, rates for eq 10

(30) King, E. L. *Int. J. Chem. Kinet.* **1982**, *14*, 1285. For a second-order reversible reaction, A + B ⇄ C + D, Δ is the displacement of a particular species from its equilibrium value. $\Delta = [A] - [A]_\infty = [B] - [B]_\infty = [C]_\infty - [C] = [D]_\infty - [D]$ and $\alpha = [A]_\infty + [B]_\infty + ([C]_\infty + [D]_\infty)/K$.

Table II. Initial Concentrations and Rate Data for Equation 9 at 20 °C

$[N \equiv Mn(TTP)]_0$ (μM)	$[Mn(OEP)]_0$ (μM)	$10^{-3}k_1$[a] (M^{-1} s^{-1})	$[N \equiv Mn(OEP)]_0$ (μM)	$[Mn(TTP)]_0$ (μM)	$10^{-3}k_{-1}$[b] (M^{-1} s^{-1})
3.39	3.40	7.7	3.29	3.36	2.2
3.56	3.54	6.2	6.67	3.36	2.6
4.03	4.45	6.6	6.58	3.36	3.0
1.13	4.54	5.4	3.89	1.95	3.4
5.49	4.83	5.6	9.71	1.95	3.3
5.00	4.86	5.5	10.4	2.10	4.1
3.00	5.74	4.4			
1.42	5.67	3.7			
3.39	6.81	5.5			

[a] Average 5.6 ± 1.2. [b] Average 3.2 ± 0.5.

Table III. Forward Rate Constants for Equation 9 in Toluene

T (°C)	$10^{-3}k_1$ (M^{-1} s^{-1})
−10	0.8 ± 0.3
0	1.5 ± 0.6
10	2.9 ± 0.3
20	5.6 ± 1.2

Table IV. Thermodynamic and Kinetic Parameters for Equation 10 in $CDCl_3$

T (°C)	K	k_1 (M^{-1} s^{-1})
22	24.3 ± 3.3	0.010 ± 0.007
30	17.5[a]	0.025 ± 0.001
40	12.2 ± 1.5	0.051 ± 0.005
50	8.7 ± 1.5	0.150 ± 0.012

[a] Extrapolated value.

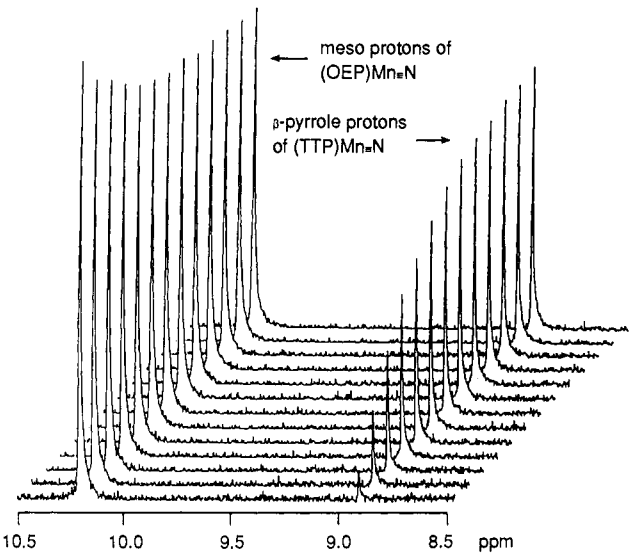

Figure 2. Stacked plot from ^1H NMR kinetics run at 40 °C showing spectra recorded at 20-min intervals. $[(OEP)Mn{\equiv}N]_0 = 3.94 \times 10^{-3}$ M, and $[(TTP)MnCl]_0 = 1.01 \times 10^{-3}$ M.

were measured by ^1H NMR spectroscopy. A typical kinetics experiment in $CDCl_3$ is shown in Figure 2. Initial concentrations used in this study ranged from 7.34×10^{-4} to 7.96×10^{-3} M. In all cases, the kinetic data were found to obey eq 8, indicating that the rate law is first order in each reactant. Rate constants are summarized in Table IV. An Eyring plot of these data yield $\Delta H^{\ddagger} = 19 \pm 2$ kcal/mol and $\Delta S^{\ddagger} = -3 \pm 6$ cal/K·mol.

To the extent allowed by metalloporphyrin solubilities, eq 10 was run under pseudo-first-order conditions to verify the nature of the rate law. For example, in an experiment run at 50 °C with a starting ratio of $[(OEP)Mn{\equiv}N]_0$:$[(TTP)MnCl]_0 = 8.5$:1 and $[(OEP)Mn{\equiv}N]_0 = 6.25 \times 10^{-3}$ M, the disappearance of [(TTP)MnCl] followed first-order kinetics for more than 2 half-lives, yielding a $k_{obs} = 8.4 \times 10^{-4}$ s^{-1}. The second-order rate constant derived from this method, $k = k_{obs}/[(OEP)Mn{\equiv}N]_0 = 0.13$ M^{-1} s^{-1}, is in good agreement with the value obtained from a direct second-order treatment (eq 8).

Table V. Monoanionic Axial Ligand Comparison for Equation 11

X	T (°C)	K	k_1 (M^{-1} s^{-1})
$(CH_3)_3CCO_2$	20	0.33 ± 0.01	$(1.3 \pm 0.1) \times 10^{-2}$[a]
Cl	22	23.5 ± 3.6	$(1.0 \pm 0.1) \times 10^{-2}$[a]
I	22	17 ± 3	5.8 ± 1.6[b]
Cl	50	8.4 ± 2.1	$(1.5 \pm 0.1) \times 10^{-1}$[a]
CH_3CO_2	50	15.4 ± 1.4	$(7.1 \pm 0.1) \times 10^{-3}$[a]

[a] In CDCl. [b] In CH_2Cl_2.

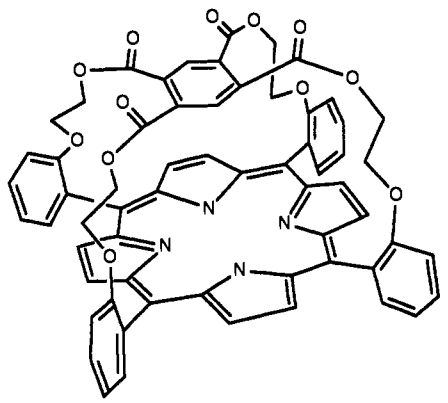

Figure 3. Structure of Baldwin's C_2-capped porphyrin.[25]

Effect of Solvent. Equation 10 was run in THF at 50 °C in an attempt to examine the influence of solvent polarity. The equilibrium constant for eq 10 in THF is $K_{eq} = 0.98$, approximately 1 order of magnitude smaller than in $CDCl_3$. A series of spectrophotometric kinetics runs were carried out in 1.0-mm cuvettes with an initial concentration of $(OEP)Mn{\equiv}N$ at 3.42×10^{-4} M. The initial concentration of (TTP)MnCl was varied from 1.18×10^{-4} to 8.82×10^{-4} M. The absorbance–time data followed the second-order integrated rate law (eq 8), yielding a rate constant of 0.10 ± 0.02 M^{-1} s^{-1}. A similar set of kinetics runs were performed in *N*-methylformamide. In this solvent, the second-order rate constant for nitrogen atom transfer between $(OEP)Mn{\equiv}N$ and (TTP)MnCl was found to be $k_1 = 20 \pm 2$ M^{-1} s^{-1}.

Effect of Axial Ligands. Axial ligand effects were studied in these systems by varying the monoanionic ligand on the starting manganese(III) porphyrin complexes as shown in eq 11. A

$$(OEP)Mn{\equiv}N + (TTP)MnX \rightleftarrows (OEP)MnX + (TTP)Mn{\equiv}N \quad (11)$$

comparison of four different axial ligands, pivalate, chloride, iodide, and acetate, is presented in Table V. The nature of the axial ligand can have a significant influence on the rate of eq 11. When chloride is replaced by iodide, a rate enhancement of 500-fold is observed at 22 °C. In contrast, substitution of chloride with acetate produces a decrease in rate by a factor of 21 at 50 °C. However, pivalato- and chloromanganese(III) complexes undergo nitrogen atom transfer at similar rates.

Reactions Involving a Sterically Encumbered Porphyrin Ligand. As a mechanistic probe, Baldwin's C_2-capped porphyrin, CAP (Figure 3), was used in place of TTP. Both TTP and CAP are

Table VI. Rate Data for Equation 12 in $CDCl_3$ at 50 °C

$[(CAP)MnCl]_0$ (M)	$[(OEP)Mn \equiv N]_0$ (M)	k_1 (M^{-1} s^{-1})
1.15×10^{-3}	2.29×10^{-3}	4.0×10^{-3}
1.12×10^{-3}	4.44×10^{-3}	3.7×10^{-3}
0.99×10^{-3}	7.88×10^{-3}	4.0×10^{-3}

Table VII. Kinetics of Equation 10 in $CDCl_3$ with Excess Cl^-

$[(OEP)Mn \equiv N]_0$ (M)	$[(TTP)MnCl]_0$ (M)	$[NBu_4Cl]$ (M)	k_1 (M^{-1} s^{-1})
1.49×10^{-3}	1.22×10^{-3}	0	$(1.50 \pm 0.12) \times 10^{-1}$
4.51×10^{-3}	1.35×10^{-3}	1.39×10^{-3}	$(1.04 \pm 0.06) \times 10^{-4}$
4.98×10^{-3}	1.48×10^{-3}	3.06×10^{-3}	$(6.55 \pm 0.14) \times 10^{-5}$

derivatives of tetraphenylporphyrin which make them similar, to a first approximation, in terms of electronic properties. Thus, the major attribute of CAP is a steric factor arising from the presence of a fifth aryl ring which blocks one face of the porphyrin. When (CAP)MnCl is treated with (OEP)Mn≡N, formation of (CAP)Mn≡N and (OEP)MnCl is observed by ^1H NMR and UV-vis spectroscopy. For example, proton NMR spectra show the decrease of the 10.29 ppm meso signal of (OEP)Mn≡N and the concomitant appearance of the two β-pyrrole proton signals (8.91 and 8.78 ppm) for (CAP)Mn≡N. Moreover, the reverse reaction, (CAP)Mn≡N plus (OEP)MnCl, also proceeds to yield (CAP)MnCl and (OEP)Mn≡N as shown in eq 12. The equilibrium constant for this process is 4.8 ± 1.8 at 50 °C in $CDCl_3$.

$$(OEP)Mn{\equiv}N + (CAP)MnCl \rightleftarrows (OEP)MnCl + (CAP)Mn{\equiv}N \quad (12)$$

The kinetic behavior of eq 12 in $CDCl_3$ at 50 °C was monitored by ^1H NMR. As in all of the previous cases, the total amount of nitrido complexes remained constant throughout the reaction as measured against Ph_3CH. Furthermore, the rate data for the capped system (eq 12) also obey the second-order integrated rate law, eq 8. In order to substantiate this kinetic order, eq 12 was run under pseudo-first-order conditions with an excess of (OEP)Mn≡N. In these cases, second-order rate constants extracted from this analysis agree to within 10% of the values determined from eq 8. Rate data for eq 12 are listed in Table VI.

Kinetics of Nitrogen Atom Transfer as a Function of Added Axial Ligand. The influence of added monoanionic axial ligands on the transfer of nitrogen between $Mn^V{\equiv}N$ and $Mn^{III}Cl$ was studied using NBu_4Cl as the external source of chloride in $CDCl_3$ solutions. The rate data from these experiments were still found to follow second-order reversible kinetics (eq 8). When $[Cl^-]$: $[(TTP)MnCl]_0$ = 1:1, rates at 50 °C decreased by a factor of 1400. A 2-fold excess of Cl^- resulted in a rate inhibition of 2600. These results are summarized in Table VII.

Discussion

We have found that nitrogen atom transfer between two metals can be extremely facile. It is possible to observe this remarkable process by using different porphyrin ligands as spectroscopic labels. An additional benefit derived from the use of metalloporphyrins arises from the structural integrity maintained by these complexes throughout the reaction. This eliminates complications due to ligand loss or stereochemical rearrangements. Because the equilibrium constant of eq 9 is near unity, nitrogen atom transfer between (TTP)Mn≡N and (OEP)Mn can be considered as a pseudo-self-exchange reaction. Consequently, the rate constant for eq 9 is a good measure of the intrinsic tendency for nitrogen atom transfer. As indicated in Table III, these rate constants are on the order of 10^3 M^{-1} s^{-1}. The temperature dependence of these rates yields activation parameters of $\Delta H^{\ddagger}$ = 9.4 ± 0.7 kcal/mol and $\Delta S^{\ddagger}$ = −10 ± 2 cal/mol·K.

Since the manganese nitrido complex, which formally contains Mn(V), is reduced to a manganese(II) complex, eq 9 represents a formal three-electron redox process. Thus, the reaction pathway for eq 9 is of great interest since it is an unprecedented process. Of fundamental concern is the issue of outer-sphere versus inner-sphere mechanisms. Insight into this question is provided by chemical studies. For example, Büchler has shown that sodium anthracenide, an outer-sphere reducing agent, is capable of adding two electrons to the porphyrin ligand of (OEP)Mn≡N, but does not reduce the metal.[31] Moreover, Bottomley has demonstrated that the first and second electrochemical reductions of (TTP)Mn≡N and (OEP)Mn≡N are ligand-based.[32] Formation of the singly reduced complexes occurs at $E_{1/2}$ = −1.10 (N≡Mn(TTP)) and $E_{1/2}$ = −1.30 (N≡Mn(OEP)) vs SCE. Since the $Mn^{III}(POR)/Mn^{II}(POR)$ reduction potentials are −0.45 V (OEP)[33] and −0.33 V (TTP)[34] vs SCE, neither Mn(OEP) nor Mn(TTP) are capable of reducing the manganese nitrido complexes in an outer-sphere process. Thus, eq 9 most likely proceeds by an inner-sphere mechanism. Furthermore, it is unlikely that eq 9 proceeds through the intermediacy of free N^{3-} ions or N atoms since these are presumably too high in energy to be involved.

Attempts to detect the putative binuclear μ-nitrido intermediate by resonance Raman or UV-vis difference spectroscopy were unsuccessful, indicating that this intermediate is present in unobservable concentrations. However, further evidence in support of a bridged intermediate is provided by the use of a coordinating solvent. For example, in THF, the rate constant for eq 9 decreases by 3 orders of magnitude. In this case, THF presumably coordinates to the Mn(II) reductant and inhibits formation of the μ-nitrido species. Further support for the coordination of THF is derived from analogous kinetic studies run in the more poorly coordinating solvent 2,5-dimethyltetrahydrofuran (cis:trans = 55:45). Accordingly, the rate constant in this medium (k_1 = 47 ± 6 M^{-1} s^{-1}) falls between those for toluene and THF. This rate is closer to the $k_{1(THF)}$ value presumably because the *cis*-2,5-dimethyltetrahydrofuran is still able to coordinate to the Mn(II) complex.

The activation parameters $\Delta H^{\ddagger}$ = 9.4 ± 0.7 kcal/mol and $\Delta S^{\ddagger}$ = −10 ± 2 cal/mol·K for eq 9 in toluene are also consistent with an inner-sphere process. The small value of $\Delta H^{\ddagger}$ suggests that significant bond formation (Mn≡N···Mn) occurs to offset the energy needed to cleave a Mn≡N triple bond. In addition, the negative entropy of activation indicates that the mechanism of eq 9 is associative in nature.

A salient result emerging from this study involves the remarkable aspect of controlling the number of redox equivalents exchanged in an electron-transfer process. By a judicious choice of substrates, nitridomanganese porphyrins can serve as either a three-electron or a two-electron oxidant. Thus, when manganese(III) porphyrins are used as the reductant, a net two-electron redox process occurs (eq 10). Few redox reagents are capable of this flexibility.[35]

A consideration of the redox chemistry of chloromanganese(III) porphyrins indicates that eq 10 does not involve an outer-sphere mechanism. Chemical and electrochemical oxidation of (TPP)MnCl produces a porphyrin-based π-cation radical.[36] The $ClMn(TPP^{\bullet+})/ClMn(TPP)$ couple occurs at $E_{1/2}$ = 1.18 V vs SCE.[37] However, the $N{\equiv}Mn(OEP)/N{\equiv}Mn(OEP^{\bullet-})$ reduction occurs at $E_{1/2}$ = −1.30 V vs SCE.[32] Thus, an outer-sphere process between N≡Mn(OEP) and ClMn(TTP) is not thermodynamically possible. Although eq 10 clearly proceeds by an inner-sphere process, it presents a more complex mechanistic situation since a double exchange of ligands (N/Cl) is involved. Both nitrido

(31) Büchler, J. W.; Dreher, C.; Lay, K.-L.; Young, J. A. L.; Scheidt, W. R. *Inorg. Chem.* **1983**, *22*, 888.
(32) Bottomley, L. A.; Neely, F. L.; Gorce, J.-N. *Inorg. Chem.* **1988**, *27*, 1300.
(33) Boucher, L. J.; Garber, H. K. *Inorg. Chem.* **1970**, *9*, 2644.
(34) Kadish, K. M.; Kelly, S. *Inorg. Chem.* **1979**, *18*, 2968.
(35) (a) Smith, E. L.; Mervyn, L.; Muggleton, P. W.; Johnson, A. W.; Shaw, N. *Ann. N.Y. Acad. Sci.* **1964**, *112*, 565. (b) Schrauzer, G. N.; Holland, H. J. *J. Am. Chem. Soc.* **1971**, *93*, 4060. (c) Balasubramanian, P. N.; Gould, E. S. *Inorg. Chem.* **1983**, *22*, 2635.
(36) (a) Spreer, L. O.; Maliyackel, A. C.; Holbrook, S.; Otvos, J. W.; Calvin, M. *J. Am. Chem. Soc.* **1986**, *108*, 1949. (b) Goff, H. M.; Phillipi, M. A.; Boersma, A. D.; Hansen, A. P. *Adv. Chem. Ser.* **1982**, *201*, 357–376. (c) Shimomura, E. T.; Phillipi, M. A.; Goff, H. M. *J. Am. Chem. Soc.* **1981**, *103*, 6778.
(37) Rodgers, K. R.; Goff, H. M. *J. Am. Chem. Soc.* **1988**, *110*, 7049.

and chloro ligands are good bridging species, and it is of fundamental interest to determine if a preference exists for a particular bridging ligand in this process.

Reactions in which Baldwin's C_2-capped porphyrin (CAP) was used in place of TTP provide unambiguous evidence for the mechanistic details of the two-electron nitrido/chloro exchange, eq 10. When the reaction is run with (CAP)Mn≡N as one of the starting complexes, backside attack trans to the nitrido ligand is prevented by the capping aromatic ring. Thus, formation of a μ-chloro intermediate cannot be an important pathway in this system. Since the reaction does proceed to yield (OEP)Mn≡N and (CAP)MnCl, it is clear that a nitrido-bridged intermediate must be involved. Furthermore, blocking the backside of the chloride complex in (CAP)MnCl does not stop the exchange process. Since metal(III) complexes of the C_2-capped porphyrin adopt a structure in which the chloride is bound to the unencumbered face of the metal,[38] an S_N2-type backside displacement of chloride cannot be involved.

Further evidence against an S_N2 mechanism can be based on a reactivity comparison of (CAP)Mn≡N and (OEP)Mn≡N. The nitride ligand is more accessible and five times more nucleophilic in (CAP)Mn≡N than in (OEP)Mn≡N.[39] Thus, in an S_N2 process, the rate of nitrogen atom transfer for (CAP)Mn≡N should be measurably faster than for (OEP)Mn≡N. However, the experimental data indicate that (CAP)Mn≡N is actually 38 times slower.

The most consistent mechanism for the Mn≡N/MnX exchange process involves an initial dissociation of the monoanionic ligand from the manganese(III) complex. Nitrogen atom transfer subsequently occurs between the cationic manganese(III) porphyrin and the nitrido complex through a μ-nitrido intermediate (Scheme I). The forward rate constant, k_f, for this mechanism

Scheme I

$$*MnCl \underset{k_{-1}}{\overset{k_1}{\rightleftharpoons}} *Mn^{III+} + Cl^-$$

$$*Mn^{III+} + Mn{\equiv}N \underset{k_{-2}}{\overset{k_2}{\rightleftharpoons}} *Mn{\equiv}N + Mn^{III+}$$

$$Mn^{III+} + Cl^- \underset{k_{-3}}{\overset{k_3}{\rightleftharpoons}} MnCl$$

Mn = (OEP)Mn *Mn = (TTP)Mn

takes the form shown in eq 13.[40] The inverse chloride dependence has been verified using tetra(*n*-butyl)ammonium chloride as an external source of Cl^- (see Table VII). Previous work has established that neutral manganese(III) porphyrin complexes, (POR)MnX, show little affinity for a sixth ligand in nonpolar solvents.[34,41] Thus, excess chloride is not likely to inhibit the reaction by taking up the sixth coordination site but must shift the initial dissociation equilibrium of Scheme I back toward (POR)MnCl. Furthermore, an S_N2-type mechanism (Scheme II) has no common ion effect as indicated by eq 14 and can be

$$k_f = k_1k_2/k_{-1}[Cl^-] \quad (13)$$

Scheme II

$$Mn^V{\equiv}N + *Mn^{III}Cl \underset{k_{-1}}{\overset{k_1}{\rightleftharpoons}} [Mn^{\cdot\cdot}N^{\cdot\cdot}*Mn]^+ + Cl^-$$

$$[Mn^{\cdot\cdot}N^{\cdot\cdot}*Mn]^+ + Cl^- \underset{k_{-2}}{\overset{k_2}{\rightleftharpoons}} ClMn^{III} + *Mn^V{\equiv}N$$

*Mn = Mn(TTP) Mn = Mn(OEP)

conclusively excluded.

$$k_f = \frac{k_1k_2[Cl^-]}{k_{-1}[Cl^-] + k_2[Cl^-]} = \frac{k_1k_2}{k_{-1} + k_2} \quad (14)$$

A pathway involving a double-bridged intermediate, A, can also be eliminated since chloride inhibition should not be observed in a mechanism involving this species. Steric factors provide further evidence against a double-bridged species. For example, if A were an important intermediate, a bulky axial ligand would inhibit the formation of A and result in a rate inhibition. However, when the larger ligand pivalate is used in place of the smaller chloride, no significant change in rate is observed (Table V).

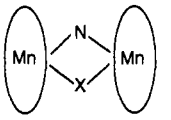

A

Solvent effects on the rate of eq 10 are also consistent with a preequilibrium dissociation of the halide from the chloromanganese(III) complex. In solvents with low dielectric constants, the rates of exchange are slow. For example, at 50 °C in $CDCl_3$ (ϵ = 4.7), the rate constant is k_1 = 0.15 M^{-1} s^{-1}. In THF, which has a similar dielectric constant (ϵ = 7.3), the rate is comparable (k_1 = 0.10 M^{-1} s^{-1} at 50 °C). However, in the much more polar solvent *N*-methylformamide (ϵ = 182), a rate enhancement of 100-fold is observed (k_1 = 20 M^{-1} s^{-1} at 50 °C). This large increase in rate is in accord with formation of a cationic [Mn(POR)]$^+$ intermediate. In fact, the ionization of (TTP)MnCl in *N*-methylformamide is clearly evident from spectrophotometric studies, particularly from the positions of bands VI and Va. In $CHCl_3$, CH_2Cl_2, and toluene, these bands appear at λ_{VI} = 375 nm and λ_{Va} = 399 nm.[42] However, in *N*-methylformamide, these bands shift to 400 and 420 nm. The red shift in these bands is characteristic of cationic manganese(III) porphyrin complexes.[43]

The mechanism proposed for the Mn≡N/MnCl exchange process (eq 10) is in stark contrast to that proposed for the irreversible heterometallic analogue Mn≡N/CrCl (eq 15).[23] In the latter process, Bottomley reports evidence in support of an S_N2-type mechanism. In this case, backside attack of the

$$(OEP)Mn{\equiv}N + (TPP)CrCl \rightarrow (OEP)MnCl + (TTP)Cr{\equiv}N \quad (15)$$

manganese nitrido complex is postulated to induce dissociation of the chloride ligand from Cr(III). This indicates that manganese(III) porphyrins are more labile than chromium(III) porphyrins. A rationale for this can be found in the electronic structure of the two reductants. The manganese(III) complex, which has a high-spin d^4 configuration, has one more electron than the high-spin d^3 Cr(III) complex. Theoretical calculations[44] indicate that this extra electron on manganese resides in a d_{z^2} orbital which is primarily Mn–Cl antibonding in character. Thus, the manganese chloro complex should be more labile than the chromium analogue.

From chemical and mechanistic studies, it is clear that the multi-electron redox processes of nitridomanganese porphyrins illustrated here involve a transient binuclear μ-nitrido intermediate. This is in stark contrast to the iron system in which the μ-nitridodiiron porphyrin complex (e.g., $[Fe(TPP)]_2N$) is thermally stable with respect to disproportionation to nitridoiron(V) porphyrin and iron(II) porphyrin complexes. An examination of the electronic structure of μ-nitridometalloporphyrin dimers provides a basis for understanding this difference. The d-orbital energy level diagram for $[Fe(TPP)]_2N$ shown in Figure 4 was derived by Tatsumi and Hoffmann using extended Hückel calculations on $[(NH_2^-)_4FeNFe(NH_2^-)_4]^{4-}$ as a computational model for the

(38) Sabat, M.; Ibers, J. A. *J. Am. Chem. Soc.* **1982**, *104*, 3715.
(39) Bottomley, L. A.; Neely, F. L. *J. Am. Chem. Soc.* **1988**, *110*, 6748.
(40) The full rate constant expression for Scheme I is $k_f = k_1k_2/(k_{-1}[Cl^-] + k_2[(OEP)Mn{\equiv}N])$. However, under the condition of excess chloride, $k_{-1}[Cl^-] \gg k_2[(OEP)Mn{\equiv}N]$ and the latter term becomes negligible.
(41) (a) Boucher, L. J. *Coord. Chem. Rev.* **1972**, *7*, 289. (b) Powell, M. F.; Pai, E. F.; Bruice, T. C. *J. Am. Chem. Soc.* **1984**, *106*, 3277.
(42) Boucher, L. J. *J. Am. Chem. Soc.* **1970**, *92*, 2725.
(43) (a) Hill, C. L.; Williamson, M. M. *Inorg. Chem.* **1985**, *24*, 2836. (b) Williamson, M. M.; Hill, C. L. *Inorg. Chem.* **1986**, *25*, 4668.
(44) (a) Zerner, M.; Gouterman, M. *Theor. Chim. Acta* **1963**, *4*, 44. (b) Gouterman, M.; Hanson, L. K.; Khalil, G.-E.; Leenstra, W. R.; Buchler, J. W. *J. Chem. Phys.* **1975**, *62*, 2343.

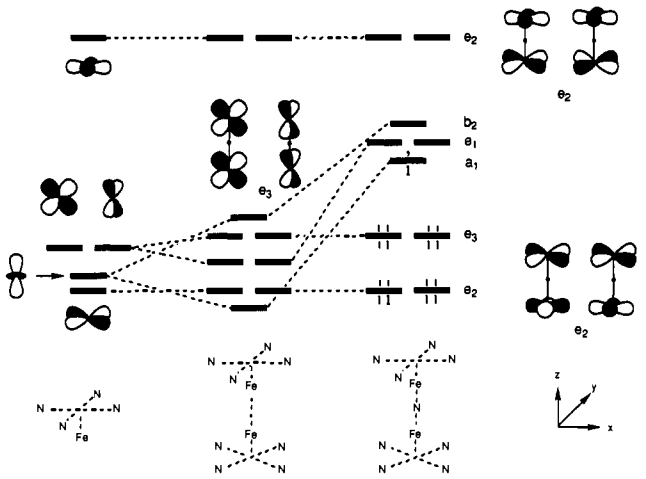

Figure 4. The building up of the orbitals of $[(NH_2^-)_4FeNFe(NH_2^-)_4]^{4-}$.[45] From left to right: the orbitals of the pyramidal N_4Fe in which Fe is displaced by 0.32 Å out of the N_4 plane; two such pyramidal N_4Fe units brought to 3.322 Å separation between the irons; the orbitals of the composite nitrido complex. The electron count shown is that appropriate to a low-spin Fe–N–Fe complex.

binuclear complex.[45] The a_1, e_1, and b_2 levels are primarily $Fe-N_{bridge}$ antibonding in character whereas the lowest energy e_2 and e_3 molecular orbitals are essentially $Fe-N_{bridge}$ nonbonding interactions. This energy level diagram correctly accounts for the ground-state electronic properties of the d^9 binuclear complex $[Fe(TPP)]_2N$. Dissociation of the μ-nitridoiron dimer is strongly disfavored because it would produce a high-energy species, (TPP)Fe≡N. Iron(V) nitrido porphyrin complexes have only been observed at low temperatures in an argon matrix and decompose above 150 K.[46] The instability of (TPP)Fe≡N has been ascribed to an electronic configuration (d^3) which necessarily contains electrons in Fe–N π^* orbitals.

To a first approximation, the energy level diagram in Figure 4 should apply to the (TTP)Mn≡N/(OEP)Mn system. Although it is not clear whether the d^7 μ-nitridomanganese dimer will adopt a high-spin or a low-spin electronic state, either case leads to the same prediction. A high-spin case would involve singly occupying the $Mn-N_{bridge}$ a_1 and e_1 antibonding levels, resulting in a strong destabilization of the μ-nitrido species. Alternatively, a low-spin state produces an electronically degenerate e_3^3 configuration. In this situation, the μ-nitrido complex is destabilized by a Jahn–Teller effect. Thus, the difference between the iron and manganese systems appears to derive largely from electronic factors.

The facility in which nitrogen atom transfer occurs between two metalloporphyrin complexes is readily understood in terms of the physical properties of the compounds involved. For example, in the three-electron Mn≡N/Mn(II) process, the oxidant (Mn≡N) is kinetically inert but contains a ligand capable of serving as a bridge. The manganese(II) porphyrin reductant has a high-spin d^5 electronic configuration which confers lability to the two axial coordination sites. Furthermore, the reductant becomes inert upon oxidation. These are important criteria for establishing an atom-transfer reaction.

Charges in coordination sphere can also play a key role in redox reactions. When large changes (≥ 2 e$^-$) in oxidation state occur, drastic reorganization of the first coordination sphere is often involved (e.g., Pt(IV)–Pt(II), V(IV)–V(II), Sn(IV)–Sn(II)). However, in metalloporphyrin complexes, the planar aromatic nature of the porphyrin ligand can greatly attenuate structural changes. In general, only modest changes in $M-N_{pyrrole}$ distances are observed. The greatest structural change typically involves displacement of the metal out of the N_4-porphyrin plane. When the complex is five-coordinate, this displacement is always toward the axial ligand. Metrical parameters for some of the manganese porphyrin complexes are listed in Table VIII.

Table VIII. Structural Comparison (Å) of Manganese Porphyrins

	$Mn-N^a_{pyrrole}$	$Mn-Ct^b$	Mn–X
Mn(TPP)[c]	2.090 (9)	0.28	
ClMn(TPP)[d]	2.008 (7)	0.27	2.363 (3)
N ≡ Mn(T*p*MPP)[e]	2.021 (2)	0.388	1.512 (2)
$[(H_2O)Mn(TPP)]SbF_6$[f]	1.995 (4)	0.19	2.105 (4)
$[(H_2O)_2Mn(TPP)]ClO_4$[f]	2.004 (2)	0	2.271 (2)

[a] Average Mn–N distance. [b] Displacement out of the N_4-porphyrin plane. [c] Gonzalez, B.; Kouba, J.; Yee, S.; Reed, C. A.; Kirner, J. F.; Scheidt, W. R. *J. Am. Chem. Soc.* **1975**, *97*, 3247. [d] Tulinsky, A.; Chen, B. M. *J. Am. Chem. Soc.* **1977**, *99*, 3647. [e] T*p*MPP is 5,10,15,20-tetrakis(*p*-methoxyphenyl)porphyrin. Hill, C. L.; Hollander, F. J. *J. Am. Chem. Soc.* **1982**, *104*, 7318. [f] Williamson, M. M.; Hill, C. L. *Inorg. Chem.* **1987**, *26*, 4155.

It is clear from Table VIII that the inner-sphere reorganization energies for nitrogen atom transfer between metalloporphyrins are likely to be small. For the three-electron process, eq 9, the ensuing change in the $Mn-N_{pyrrole}$ distance is on the order of 0.07 Å. The greatest structural change involves a Mn out-of-plane displacement of 0.11 Å. The nitrogen atom transfer reaction of (POR)Mn≡N with $(POR)Mn^{II}$ thus involves an economy of motion in which the bridging nitrogen moves from Mn(V) to Mn(II) without requiring any other significant nuclear motion.

Concluding Remarks

A number of significant results have evolved from this study. Of primary importance is the demonstration that a terminally bound nitrido ligand can serve as a good bridging species in electron-transfer processes. Furthermore, it is possible to vary the number of redox equivalents exchanged in an atom-transfer process by choosing an appropriate substrate. In the reactions examined here, nitrogen atom transfer can mediate both three- and two-electron processes. When given a choice of potential bridging ligands (e.g., N vs Cl, I, acetate, or pivalate) the multi-electron processes studied here preferentially select the multiply bonded ligand. It is thus clear that, in utilizing what have long been considered to be thermodynamically robust metal–nitrido complexes, consideration must be given to the lability of these systems.

Acknowledgment. Financial support for this work was provided by the Research Corporation and a University Research Grant administered by Iowa State University. L.K.W. acknowledges support from the NSF in the form of a PYI award. We thank Dr. B. Rospendowski and Professor Therese Cotton for running the resonance Raman studies and Dr. M. R. Maurya for synthesizing the C_2-capped porphyrin.

(45) (a) Tatsumi, K.; Hoffmann, R.; Whangbo, M.-H. *J. Chem. Soc., Chem. Commun.* **1980**, 509. (b) Tatsumi, K.; Hoffmann, R. *J. Am. Chem. Soc.* **1981**, *103*, 3328.

(46) (a) Wagner, W.-D.; Nakamoto, K. *J. Am. Chem. Soc.* **1988**, *110*, 4044. (b) Wagner, W.-D.; Nakamoto, K. *J. Am. Chem. Soc.* **1989**, *111*, 1590.